Fig. 7.3. Shock or detonation polars can be used in conjunction with polar representations of other wave processes to illustrate the graphical solution of numerous two-dimensional wave interaction problems.

This procedure enables the use of our computational tools discussed in Section 8 for normal waves but any method (such as Reynolds (1986) or Gordon and McBride (1976)) to solve the jump equations can be used to generate solutions for oblique waves without having to make any assumptions regarding the specific heats, energy release or equilibrium compositions. As long as the material can be treated as a fluid (for example, solids at sufficiently high pressure), this technique can be used. Once a shock adiabat is determined in the form $w_2 = f(w_1)$, solutions for any upstream velocity can be obtained readily by these simple transformations. This procedure is not restricted to ideal gases and can be used on any substance for which the hydrodynamic model of shock waves applies, for example, strong shocks in solids or liquids.

7.4 Prandtl-Meyer Expansion

In steady supersonic flow with a uniform upstream state, an expansion wave turns the flow and is accompanied by an isentropic expansion. The amount of turning $\mathrm{d}\theta$ and the change in flow speed $\mathrm{d}u$ are related by Liepmann and Roshko (1957), Thompson (1972)

$$\mathrm{d}\theta = \pm\sqrt{M^2-1}\frac{\mathrm{d}u}{u}\,, \tag{7.52}$$

where the flow Mach number $M = u/a$ and in an expansion turn $\mathrm{d}u > 0$. The two signs correspond to the two possible changes in direction as measured from the incoming flow direction. For example, in Figure 7.4, the minus sign is appropriate. The expansion wave in this situation is bounded by the characteristics or *Mach lines* which are at angle $\mu = \sin^{-1}(1/M)$ to the flow; this angle always decreases across the expansion wave as M increases. The quantity on the right-hand side of (7.52) defines the *Prandtl-Meyer* function ω by

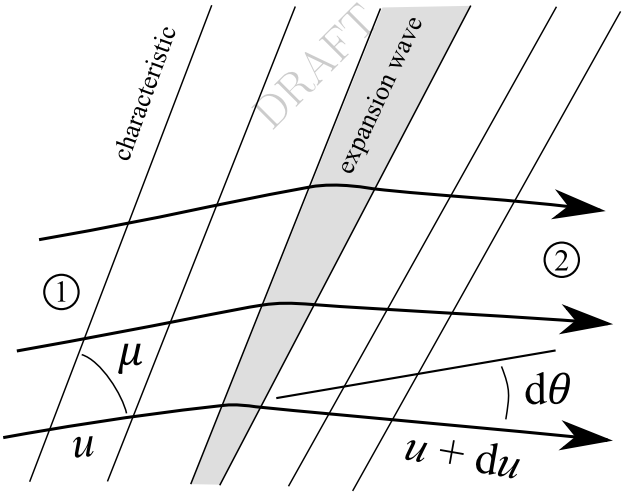

Figure 7.4: Illustration of an expansion fan between two uniform states, 1 and 2, deflecting the flow downward $\mathrm{d}\theta < 0$ and increasing the speed $\mathrm{d}u > 0$

the differential expression

$$\mathrm{d}\omega = \sqrt{M^2-1}\frac{\mathrm{d}u}{u} \tag{7.53}$$

An analytic expression for $\omega(M)$ can be computed for perfect gases, see Appendix A.10, and can be determined numerically for real gases through integration following appropriate transformation of the right-hand side, presented next.

Along a streamline in adiabatic flow, the total enthalpy is constant

$$h_t = h + \frac{1}{2}u^2\,. \tag{7.54}$$

For streamlines passing through an isentropic expansion wave and originating in a uniform state, the entropy s will also be constant $s_\circ$ so that the enthalpy and therefore the velocity are a function of only one thermodynamic variable, for example, mass density ρ.

$$u = \sqrt{2(h_t - h(s_\circ, \rho))} \; . \tag{7.55}$$

The sound speed is defined by

$$a^2 = \left(\frac{\partial P}{\partial \rho}\right)_s \tag{7.56}$$

and is also a function only of density in isentropic flow, $a = a(s_\circ, \rho)$. The Mach number can then be computed as a function of density

$$M = \frac{u}{a} = \frac{\sqrt{2(h_t - h(s_\circ, \rho))}}{a(s_\circ, \rho)} \; . \tag{7.57}$$

The change in flow velocity itself can be expressed in terms of the thermodynamic changes by using the momentum equation for the flow on the streamline

$$\rho u \mathrm{d}u = -\mathrm{d}P \; . \tag{7.58}$$

Using the definitions of sound speed and Mach number, for isentropic flow along a streamline, this is equivalent to

$$\frac{\mathrm{d}u}{u} = -\frac{1}{M^2}\frac{\mathrm{d}\rho}{\rho} \tag{7.59}$$

Finally, we obtain an expression suitable for numerical integration of $\mathrm{d}\omega$

$$\mathrm{d}\omega = -\frac{\sqrt{M^2 - 1}}{M^2}\frac{\mathrm{d}\rho}{\rho} \qquad \text{where} \qquad M^2 = \frac{2(h_t - h(s_\circ, \rho))}{a^2(s_\circ, \rho)} \tag{7.60}$$

An example of using this procedure for the equilibrium expansion of hot air (3000 K and 1 atm initial conditions) is implemented in demo_PrandtlMeyer.m. and some representative results are shown in Fig 7.5.

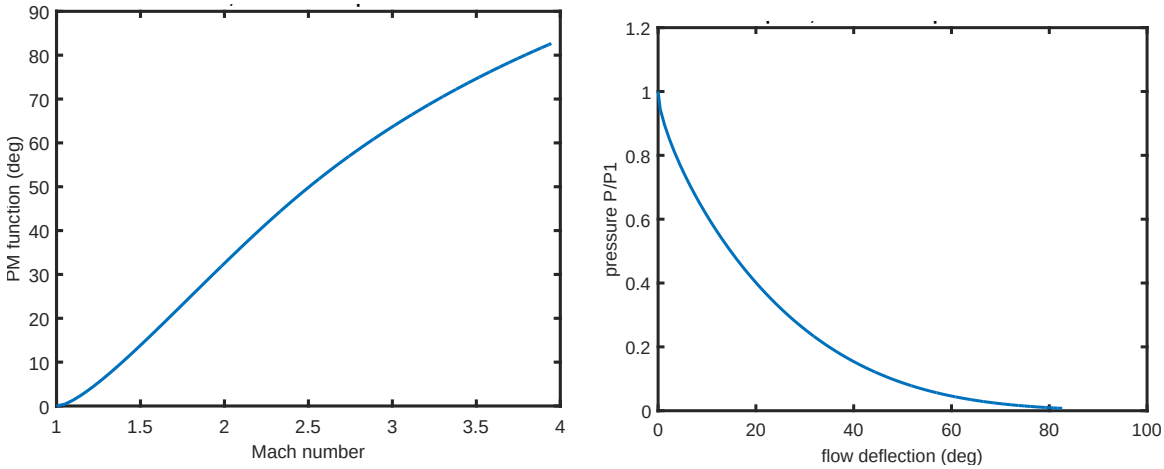

(a) (b)

Figure 7.5: Example results from numerical evaluation of Prandtl-Meyer function for equilibrium expansion of hot air (3000 K and 1 atm initial conditions). (a) Prandtl-Meyer function $\omega(M)$. (b) Pressure-deflection $P(\theta)$ relationship within expansion fan.

7.5 Isentropic Expansion Following Shock Wave

The interaction of shock waves with material interfaces can generate a reflected expansion wave (Meyers, 1994, Glass and Sislian, 1994). In order to calculate the strength of this wave, it is necessary to find the states on the isentrope passing through the post-shock state and values of the Riemann function. The program shock_state_isentrope.m computes the shock state for a specified shock speed and calculates states on the isentrope. The output is a file `shock_isentrope.txt` containing the v, T, P, a_{eq}, u evaluated at fixed intervals on the isentrope. The example is for a shock wave in air with a speed of 1633 m/s. The initial conditions are:

```
# Shock State Isentrope
# Calculation run on 29-Jan-2008 05:47:49
# Initial conditions
# Shock speed  (m/s) 1633.0
# Temperature (K) 295.0
# Pressure (Pa) 100000.0
# Density (kg/m^3) 1.1763e+000
# Initial species mole fractions: N2:3.76 O2:1.0
# Reaction mechanism: gri30_highT.cti
```

and the results are shown in Fig. 7.6.

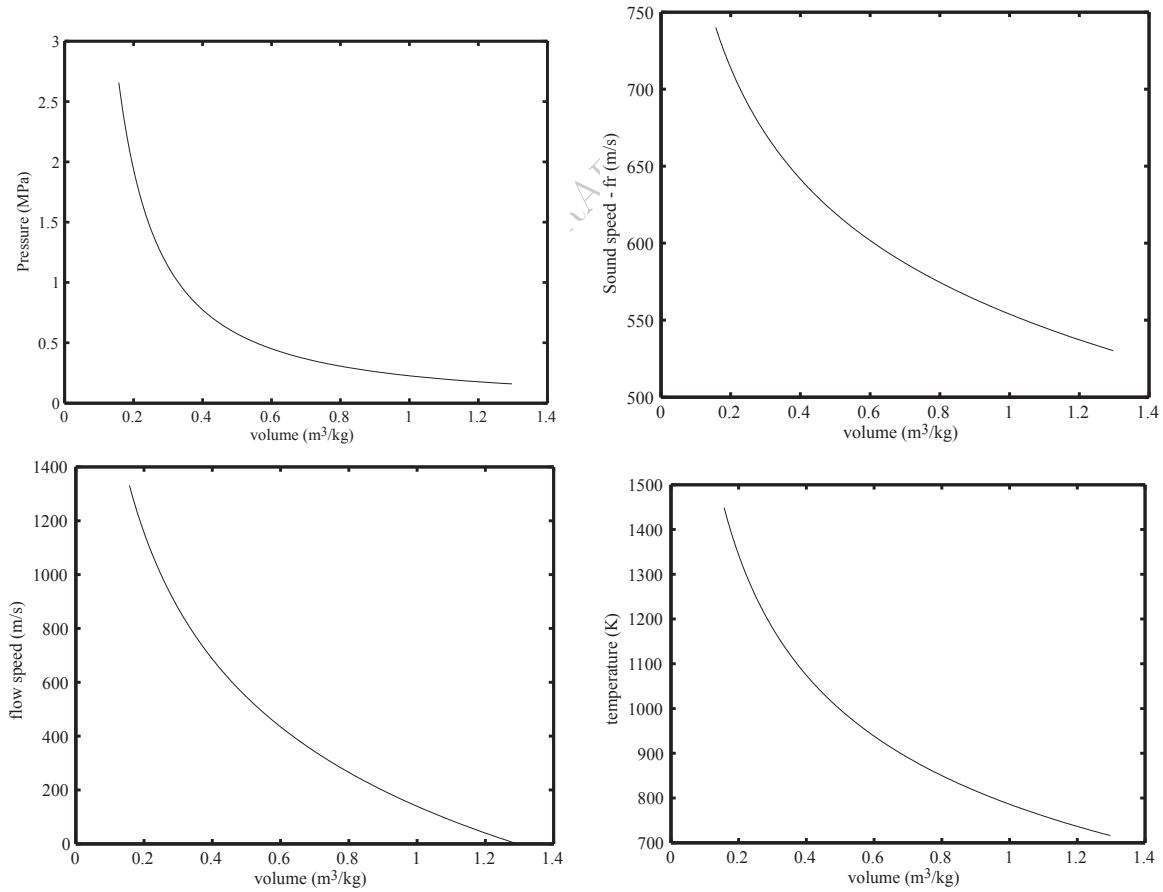

Figure 7.6: Property variation on an isentrope (frozen) passing through the postshock state of a 1633 m/s shock wave in air.

7.6 Reflection of overdriven detonation waves

Detonation waves emerging from a deflagration-to-detonation transition event (Ciccarelli and Dorofeev, 2008, Breitung et al., 2000) are often observed to have a velocity in excess of the Chapman-Jouguet speed for that mixture, $U > U_{CJ}$. Such waves are referred to as overdriven and the peak pressure produced by wave reflection from a closed end is of interest in estimating structural loads. The estimation of peak pressure behind both incident and reflected waves is straightforward using the programs described in Section 6.4 and 6.6. An example program in MATLAB is given in demo_overdriven.m which computes the states behind incident and reflected waves in H_2-N_2O mixtures as a function of wave speed and prints a summary `overdriven_reflection.txt` output file. A plot of the incident and reflected pressures from the output file is shown in Fig. 7.7. The ratio of reflected-to-incident pressure (Fig. 7.8) varies from about 2.4 for the CJ detonation up to 6.5 for a highly overdriven wave. The increase in pressure ratio with wave speed shows that as the wave speed increases, the combustion energy release becomes less important than the kinetic energy in the flow

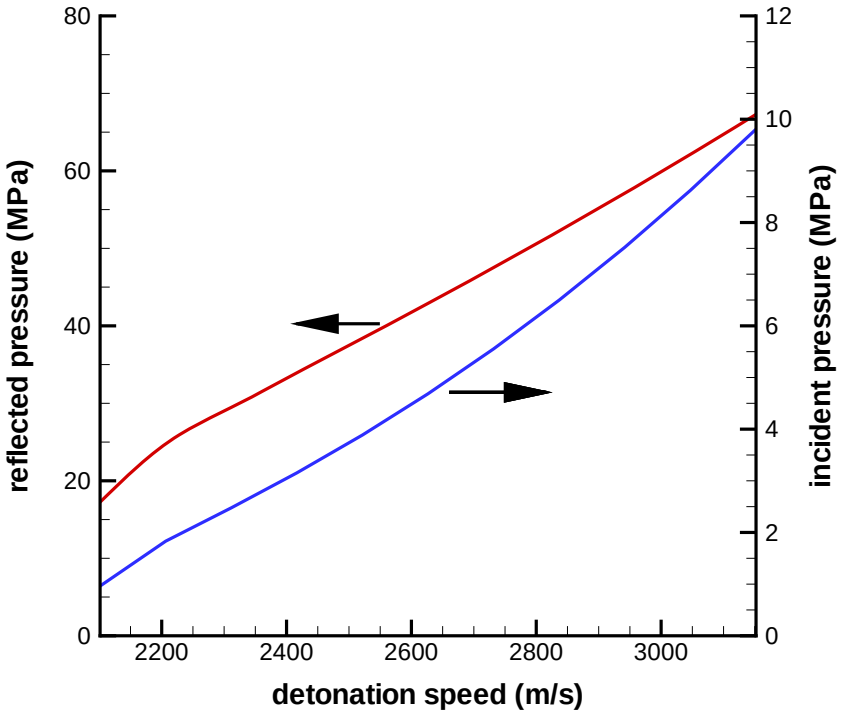

Figure 7.7: Incident and reflected pressures for a detonation in H_2-N_2O (31% H_2, 1 bar , 300 K) mixtures.

7.7 Detonation in a compressed gas region and subsequent reflection

Detonation in a closed vessel or pipe can occur after a deflagration (flame) is ignited, then accelerates to high speed and transitions to detonation near the vessel surface or the closed end of the pipe (Shepherd, 1992). The initial deflagration propagates quite slowly and results in the compression of the unburned gas ahead of the wave as the pressure increases inside the vessel. As a consequence, the detonation occurs in a compressed gas region which has higher pressure and temperature than the initial gas within the vessel. In addition, the detonation may emerge from the transition region with a much higher velocity and pressure than the CJ values. This results in much higher detonation pressures behind the reflected shock wave created when the detonation reaches the vessel wall or pipe end. The MATLAB script precompression_detonation.m. computes the conditions behind a CJ detonation wave and associated reflected shocks in an isentropically

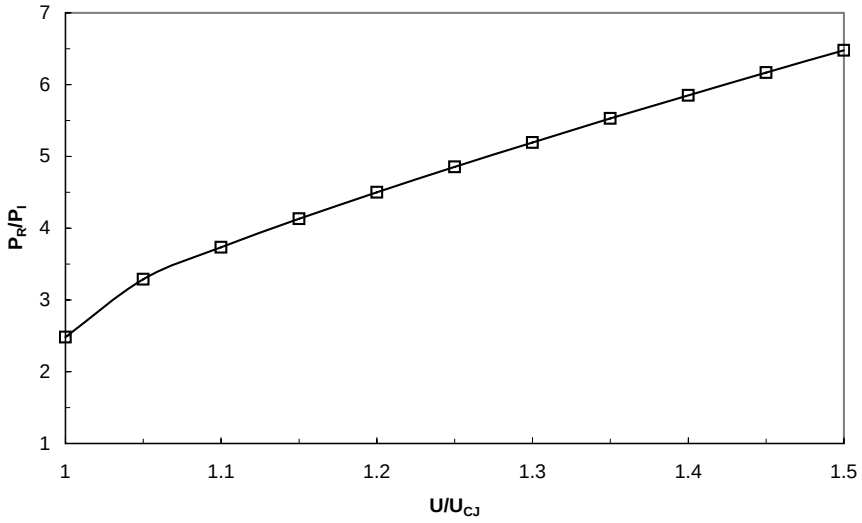

Figure 7.8: Ratio of reflected-to-incident pressures for data in Fig. 7.7.

compressed gas for a range of compression ratios. The pressures behind overdriven detonation waves and associated reflected shocks is then computed for each isentropic compression condition. The results are given in an `precompressed_detonation_reflection.txt` output file.

7.8 Pressure-velocity relationship behind a detonation

Interaction of a detonation wave or a shock with a contact surface will result in reflected and transmitted waves (Meyers, 1994, Glass and Sislian, 1994). The computation of these wave amplitudes (for a one-dimensional interaction) requires matching pressure and velocity at the contact surface. This requires computing the locus of shock and expansion wave states "centered" on the state behind the incident detonation wave or shock. This can be carried out by combining the methods that have been previously developed to compute the conditions behind the incident shock and then the subsequent shock or expansion moving into that state. A MATLAB script detonation_pu.m. computes the conditions behind a CJ detonation wave and the pressure-velocity relationship for a shock wave moving back into the detonation products. The output from the script is in a `cj-pu.txt` file that can be used to construct a pressure-velocity diagram. An example for a detonation in H_2-N_2O is shown in Fig. 7.9a. The case of a shock wave is appropriate for a reflection from "hard" material, that is, one that has a higher acoustic impedance than the material in the post-shock or post-detonation state. The solution to the interface matching condition requires constructing the pressure-velocity relationship for the "hard" material and finding the intersection. An example for a detonation wave incident on water is shown in Fig. 7.9b. Water is quite stiff and dense in comparison to the detonation products so that the interface pressure is very close to that found for rigid reflection ($u = 0$) and only a small velocity (4 m/s) is induced.

7.9 Ideal Rocket Motor Performance

The performance of an ideal rocket motor can be described by the quasi-one dimensional steady flow relationships. In general, accurate estimates of performance require consideration of the kinetics of the reactions in the gases in order to predict the extent of recombination and exhaust velocity at the exit of the nozzle. In realistic engineering design we need to also consider two- and three-dimensional flow, boundary layers, heat transfer, and most importantly, off-design operation with shock waves inside the nozzle that result in flow separation and recirculation. These effects are all outside the scope of quasi-one dimensional flow and the present discussion is only considered with ideal nozzle performance, which can be bounded by considering

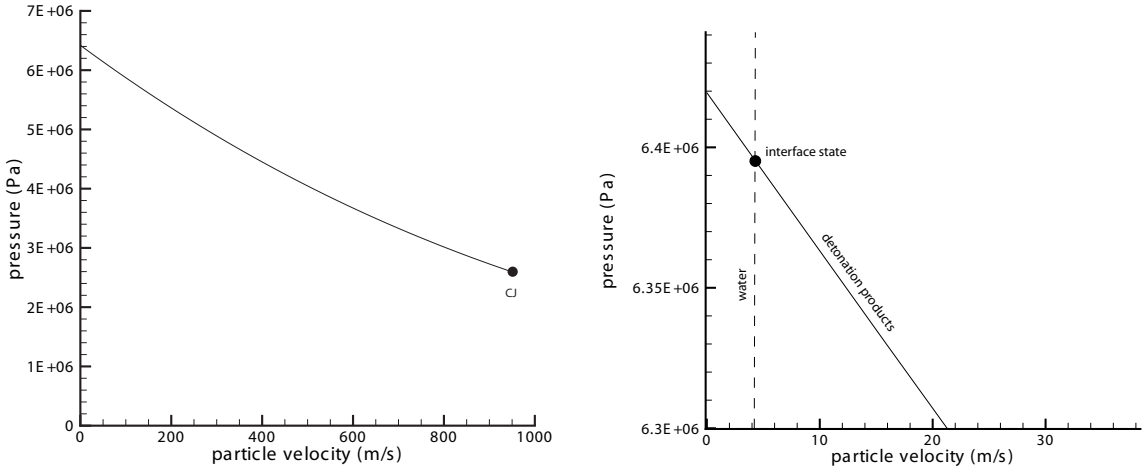

(a) (b)

Figure 7.9: a) CJ state and pressure velocity-relationship on reflected shock wave for H_2-N_2O mixtures initially at 300 K and 1 bar. b) Matching pressure and velocity for transmitting a shock wave into water.

the simple limiting cases of either *frozen* or *equilibrium* isentropic expansion within an inviscid stream tube of specified area.

The conditions inside the combustion chamber are estimated by carrying out a constant-pressure equilibrium computation using the specified inlet conditions and mixture of fuel and oxidizer to determine the initial enthalpy. Neglecting the velocity of the bulk flow within the chamber, the enthalpy of the combustion products is taken to be the total (ideal stagnation) enthalpy and the chamber pressure is the total pressure. With these as initial conditions, the flow in the nozzle is computed using the ideal quasi-one dimensional model.

In steady, quasi-one dimensional flow, the mass flow rate is constant

$$\rho u A = \dot{M} \tag{7.61}$$

$$= \text{constant} , \tag{7.62}$$

and equal to the values at the sonic point which is the location of the ideal throat in the converging-diverging nozzle downstream of the combustion chamber.

$$= \rho^* u^* A^* \quad \text{where} \quad u^* = a . \tag{7.63}$$

The total enthalpy is constant

$$h_t = h + \frac{u^2}{2} \tag{7.64}$$

so that the velocity can be computed from the thermodynamic state as

$$u = \sqrt{2(h_t - h)} . \tag{7.65}$$

The enthalpy is considered to be a function of pressure, entropy, and composition

$$h = h(P, s, \ \mathbf{Y}) \tag{7.66}$$

The entropy is fixed at the value of the products in the combustion chamber and the composition is either specified to be the state in the combustion chamber (frozen flow)

$$Y_{i,fr} = Y_i \quad \text{combustion products in chamber} \tag{7.67}$$

or computed to be the equilibrium state consistent with the given pressure at fixed entropy

$$Y_{i,eq} = Y_i(P, s = s_{chamber}) \quad \text{equilibrium at specified } P,\ s\ . \tag{7.68}$$

The ideal thrust for expansion to a given area, velocity, and pressure is

$$F = \dot{M}u + A(P - P_a) \tag{7.69}$$

which is traditionally expressed as the specific impulse, defined as

$$I_{sp} = \frac{F}{\dot{M} g_e} \tag{7.70}$$

$$= \frac{u}{g_e} + \frac{P - P_a}{\rho u g_e} \tag{7.71}$$

where P_a is the ambient pressure and $g_e = 9.81$ m·s^{-2} is the acceleration of gravity on the earth's surface. The vacuum performance is obtained when $P_a \to 0$. In practice, the lowest pressure that can be used in the computation is limited by the temperature range of the thermodynamic fitting polynomials (usually valid only to 200 K) and the convergence of the numerical solution to the isentrope.

An example of the computation of flow in a nozzle is given in the MATLAB program demo_quasi_1d.m for a hydrogen-oxygen-helium mixture with varying amounts of helium. This program uses interpolation to find the throat conditions and recalculates the streamtube area as the nondimensional value A/A^*. A modification of this program rocket_impulse.m computes and plots (Fig. 7.10) an estimate of the vacuum I_{sp} for both frozen and equilibrium conditions.

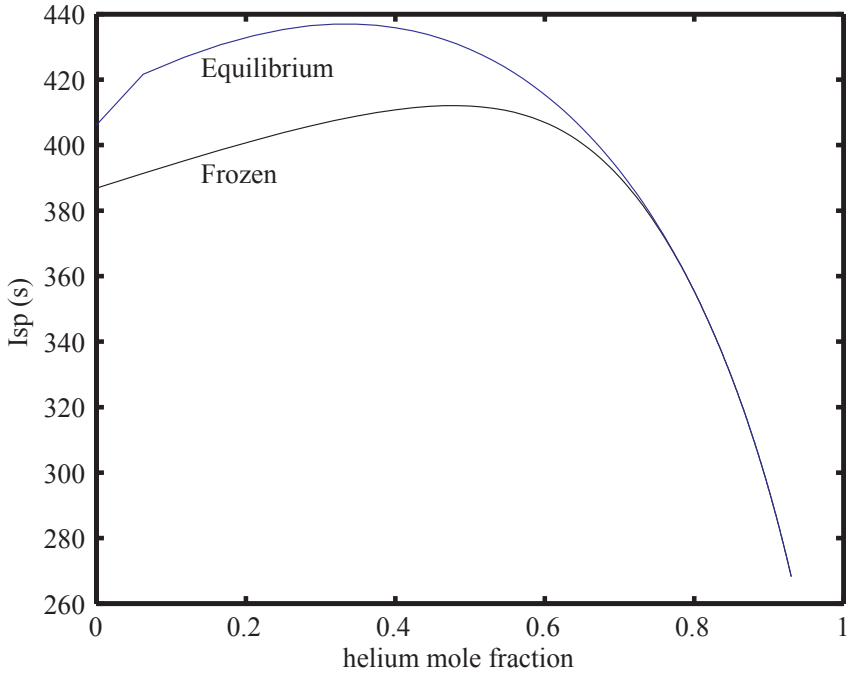

Figure 7.10: Vacuum specific impulse for an ideal hydrogen-oxygen-helium rocket motor

7.10 Equilibrium and Frozen Isentrope Properties

Computation of compressible reactive flows is often simplified by considering portions of the flow to satisfy equilibrium or frozen conditions and approximating the equation of state by simple analytical forms based

on perfect gases. In regions that are free from shock waves, inviscid adiabatic flow is treated as isentropic although the entropy may differ on adjacent streamlines. The variation of properties on isentropes such as sound speed, Grüneisen parameter, ratio of specific heats and logarithmic slopes requires the computation of derivatives. These derivatives can be found analytically for ideal gases frozen composition but for equilibrium compositions, the derivatives must be computed numerically.

The computation of the isentropes and derivatives is described in this appendix. The demonstration program demo_g.m shows how to implement the methods for numerical evaluation described in the following sections. Graphical results are shown for a simple example of isentropic expansion along an isentrope (frozen and equilibrium) from the constant volume explosion state of a stoichiometric H_2-O_2 mixture initially at conditions of 1 atm and 300 K.

Isentropes

The computations of the isentropes is straightforward, requiring the specification of the entropy and one other thermodynamic variable such as temperature, pressure or specific volume. Either the frozen or equilibrium state is evaluated at this condition, using the appropriate gas composition. Once the state is determined, then all thermodynamic properties can be evaluated.

Given an entropy value $S2$, a composition $X2$ and a specific volume V, the computation of equilibrium and frozen isentropes proceeds as follows:

```
% equilibrium state
set(gas,'V',V,'S',S2);
equilibrate(gas,'SV');
P(i) = pressure(gas);
T(i) = temperature(gas);
% frozen state
set(gas,'S',S2,'V',V,'X',X2);
P_f(i) = pressure(gas);
T_f(i) = temperature(gas);
```


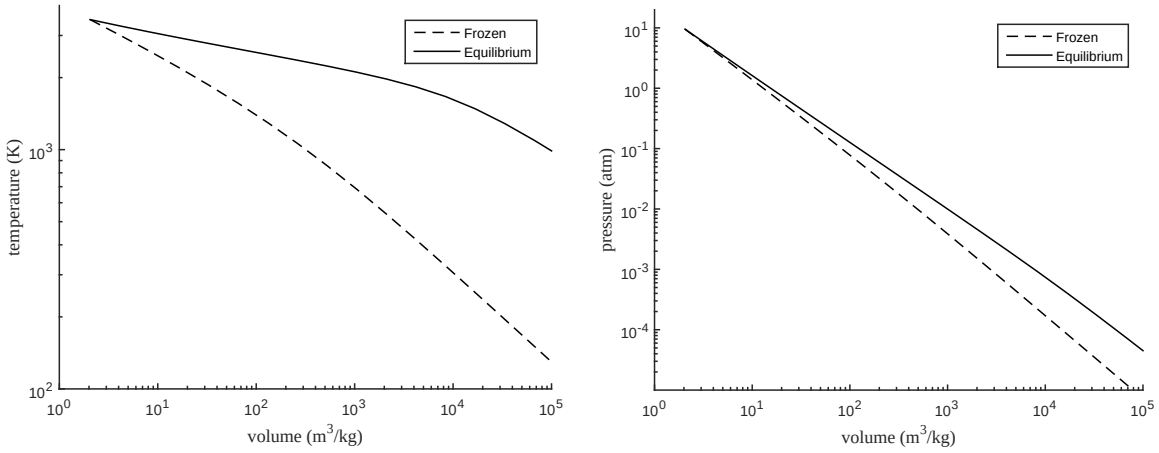

(a) (b)

Figure 7.11: (a) Frozen vs. equilibrium isentrope in P-V coordinates. (b) Frozen vs. equilibrium isentrope in P-V coordinates. Values are for isentropic expansion of combustion products of a stoichiometric H_2-O_2 constant volume explosion with initial state of 1 atm and 300 K.

From these plots it is clear that one of the key differences between frozen and equilibrium isentropes is that at the same volume, the temperature of the equilibrium isentrope is much higher than the frozen isentrope. This is due to the thermal energy released by recombination of the dissociated combustion products with

decreasing temperature (increasing volume). On the other hand, the frozen and equilibrium pressures show much smaller differences than temperatures at a given volume. Another key difference is that the slope of equilibrium sound speed in $P - V$ coordinates is less negative than the slope of the frozen sound speed. While it is not obvious, it is possible to show on general thermodynamic grounds that this is always true. This has implications for the sound speed as discussed in the next section. For both equilibrium and frozen states, the curvature of the temperature-volume relation in log-log coordinates indicates that a power-law (polytropic) fit will be inaccurate over a large range of volumes. This curvature is due to the combined effects of specific heat and in the case of equilibrium, composition, dependence on thermodynamic state.

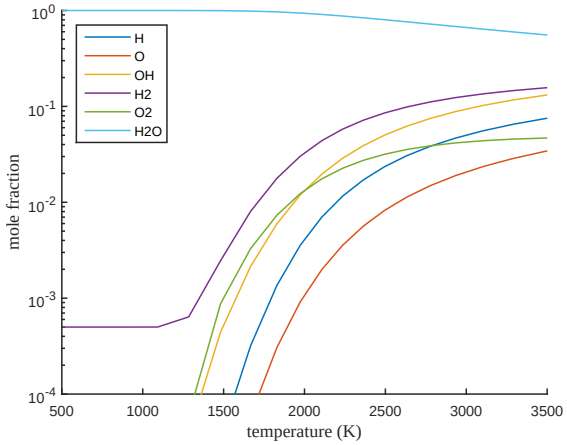

Figure 7.12: Species equilibrium composition on the isentrope for the case described in Fig. 7.11.

For a limited range of states, a standard engineering representation of the isentropes is a polytropic approximation:

$$Pv^k = P_1 v_1^k = \text{constant} \; ; \tag{7.72}$$

$$Tv^{k'-1} = T_1 v_1^{k'-1} = \text{constant} \; ; \tag{7.73}$$

where the constants k and k' are determined by fitting the exact results shown in Fig. 7.11. The range of the volumes has to be limited in order to get reasonable bounds for the exponents. Limiting the fits to $v \leq 1000 v_1$, the following values of the exponents are obtained (see demo_g.m):

$$k_{fr} = 1.2597 \; ; \tag{7.74}$$

$$k_{eq} = 1.1075 \; ; \tag{7.75}$$

$$k'_{fr} = 0.2597 \; ; \tag{7.76}$$

$$k'_{eq} = 0.08016 \; ; \tag{7.77}$$

For a perfect gas with a constant ratio of specific heats

$$\gamma = c_p / c_v \; , \tag{7.78}$$

the exponents are given by

$$k = \gamma \; , \tag{7.79}$$

$$k' = \gamma - 1 \; . \tag{7.80}$$

The relationship $k' = k - 1$ is numerically satisfied to four significant figures in the frozen case but the value of k'_{eq} in the equilibrium case is 20% lower than $k_{eq} - 1$. The fit-derived value of $k_{fr} - 1$ obtained for the frozen case is about 18% higher than the average of the frozen thermodynamic values of $\gamma \approx 1.2119$ in the range of fitted volumes. The discrepancy in numerical values between k_{fr} and γ_{fr} is due to fitting the data in log-log coordinates with a linear model over a large range of specific volume.

Sound Speed

The starting point for our computation of equilibrium sound speed is the expression that is usually taken to define sound speed in terms of its squared value:

$$a^2 = \left(\frac{\partial P}{\partial \rho}\right)_s \ . \tag{7.81}$$

If the thermodynamic state is constrained to be equilibrium then the derivative is interpreted as being the slope of the equilibrium isentrope in P-ρ coordinates

$$a^2_{eq} = \left(\frac{\partial P}{\partial \rho}\right)_{s,\ \mathbf{Y}^{eq}} \ . \tag{7.82}$$

An alternative expression for sound speed that is used in compressible flow is in terms of derivatives of enthalpy $h(P, \rho,\ \mathbf{Y})$.

$$\mathrm{d}h = \left(\frac{\partial h}{\partial P}\right)_{\rho,\mathbf{Y}} \mathrm{d}P + \left(\frac{\partial h}{\partial \rho}\right)_{P,\ \mathbf{Y}} \mathrm{d}\rho + \sum_{i=1}^{k} \left(\frac{\partial h}{\partial Y_i}\right)_{P,\rho,Y_{j\neq i}} \mathrm{d}Y_i \tag{7.83}$$

For equilibrium flow $\mathbf{Y} = \mathbf{Y}^{eq}(P, \rho)$ and

$$\mathrm{d}Y_i^{eq} = \left(\frac{\partial Y_i^{eq}}{\partial P}\right)_{\rho,Y_{j\neq i}} \mathrm{d}P + \left(\frac{\partial Y_i^{eq}}{\partial \rho}\right)_{P,Y_{j\neq i}} \mathrm{d}\rho \ . \tag{7.84}$$

The fundamental relation of thermodynamics can be written

$$\mathrm{d}h = T\,\mathrm{d}s + \frac{\mathrm{d}P}{\rho} + \sum_{i=1}^{k} \mu_i\,\mathrm{d}n_i \tag{7.85}$$

The last term vanishes for either frozen or equilibrium processes. Eliminating $\mathrm{d}h$ between these two expressions we have for frozen flow

$$a^2_{fr} = \frac{\left(\frac{\partial h}{\partial \rho}\right)_{P,\ \mathbf{Y}}}{\frac{1}{\rho} - \left(\frac{\partial h}{\partial P}\right)_{\rho,\ \mathbf{Y}}} \ . \tag{7.86}$$

and for equilibrium flow

$$a^2_{eq} = \frac{\left(\frac{\partial h}{\partial \rho}\right)_{P,\ \mathbf{Y}} + \sum_{i=1}^{k} \left(\frac{\partial h}{\partial Y_i}\right)_{P,\rho,Y_{j\neq i}} \left(\frac{\partial Y_i^{eq}}{\partial \rho}\right)_{P,Y_{j\neq i}}}{\frac{1}{\rho} - \left(\frac{\partial h}{\partial P}\right)_{\rho,\ \mathbf{Y}} - \sum_{i=1}^{k} \left(\frac{\partial h}{\partial Y_i}\right)_{P,\rho,Y_{j\neq i}} \left(\frac{\partial Y_i^{eq}}{\partial P}\right)_{\rho,Y_{j\neq i}}} \ , \tag{7.87}$$

which can be written as

$$a^2_{eq} = \frac{\left(\frac{\partial h^{eq}}{\partial \rho}\right)_{P}}{\frac{1}{\rho} - \left(\frac{\partial h^{eq}}{\partial P}\right)_{\rho}} \ . \tag{7.88}$$

where

$$\left(\frac{\partial h^{eq}}{\partial \rho}\right)_P = \left(\frac{\partial h(P,\rho,\mathbf{Y}^{eq}(P,\rho))}{\partial \rho}\right)_P \tag{7.89}$$

and

$$\left(\frac{\partial h^{eq}}{\partial P}\right)_\rho = \left(\frac{\partial h(P,\rho,\mathbf{Y}^{eq}(P,\rho))}{\partial P}\right)_\rho . \tag{7.90}$$

Although not obvious from (7.83) and (7.87), it is possible to show on general thermodynamic grounds (see Appendix 4D Fickett and Davis, 1979) that the equilibrium sound speed will always be less than the frozen sound speed.

$$a_{fr} \geq a_{eq} \tag{7.91}$$

The holds irrespective of the nature of the equilibration process, endothermic or exothermic. This inequality is a consequence of the extremum properties of equilibrium processes, discussed in Chapter 4.

Provide a derivation of (7.91) using thermodynamic transformation to reaction coordinates and properties of the Hessian at the equilibrium state.

Numerical computation of sound speed

A simple finite difference approach to computing the sound speed is to evaluate pressure at two states, 1 and 2, at nearby points on an isentrope and to form the difference quotient

$$\frac{df}{dx} \approx \frac{f(x_2) - f(x_1)}{x_2 - x_1} \tag{7.92}$$

If we select the two points to be equally spaced about a central point x_0, $x_1 = x_0 - h$ and $x_2 = x_0 + h$, then we recover the central difference approximation to the first derivative

$$\left.\frac{df}{dx}\right|_{x_0} = \frac{f(x_0+h) - f(x_0-h)}{2h} + \mathcal{O}(h^2) , \tag{7.93}$$

which as indicated, is accurate to second order in the increment h. Applying this to the computation of (7.82) and considering $P(\rho, s,\ \mathbf{Y})$ we obtain

$$a_{eq}^2 \approx \frac{P(\rho_0 + \Delta\rho, s_0,\ \mathbf{Y}^{eq}) - P(\rho_0 - \Delta\rho, s_0,\ \mathbf{Y}^{eq})}{2\Delta\rho} , \tag{7.94}$$

where the equilibrium composition $\mathbf{Y}^{eq}$ is evaluated at the entropy and density associated with that state.

A straightforward implementation of this approach is to start with an initial equilibrium state and then to use the `'SV'` option to perform equilibrium computations of adjacent states at a fixed entropy and two density values. The MATLAB code soundspeed_eq.m that implements this approach is:

```
rho0 = density(gas);
T0 = temperature(gas);
p0 = pressure(gas);
s0 = entropy_mass(gas);
x0 = moleFractions(gas);
rho1 = 0.99*rho0;
set(gas,'Density',rho1,'Entropy',s0,'MoleFractions',x0);
equilibrate(gas,'SV');
p1 = pressure(gas);
rho2 = 1.01*rho0;
set(gas,'Density',rho2,'Entropy',s0,'MoleFractions',x0);
```

```
equilibrate(gas,'SV');
p2 = pressure(gas);
dpdrho_s = (p2 - p1)/(rho2 - rho1);
aequil = sqrt(dpdrho_s);
set(gas,'Temperature',T0,'Pressure',p0,'MoleFractions',x0);
```

If the reference state passed to the function in the gas object is not in equilibrium, the result of the call is still valid but requires care in interpretation. The resulting equilibrium sound speed is based on an equilibrium isentrope that passes through the (S, V) state that is passed to the function but composition and therefore the thermodynamic properties such as pressure and temperature will be quite different from those of the reference state.

The approach outlined above is useful for most cases but there are reference states that are challenging for the Cantera equilibrium solver to converge when using the `'SV'` option. The Cantera equilibrium solver is optimized and most robust when used in the `'TP'` mode. To take advantage of this, consider variations in entropy with small changes in temperature and pressure

$$s = s_0 + \left(\frac{\partial s}{\partial T}\right)_P \Delta T + \left(\frac{\partial s}{\partial P}\right)_T \Delta P + \dots \ . \tag{7.95}$$

In this expression and what follows, the constraint of equilibrium is not explicity stated. On an isentrope, $s = s_0$ and dropping the higher order terms, we obtain the following relationship between small temperature and pressure changes along the isentrope

$$\Delta T = -\frac{\left(\frac{\partial s}{\partial P}\right)_T}{\left(\frac{\partial s}{\partial T}\right)_P} \Delta P \ , \tag{7.96}$$

which can also be written as

$$= \left(\frac{\partial T}{\partial P}\right)_s \Delta P \tag{7.97}$$

The two derivatives on the right-hand side of (7.96) can be computed using centered differences,

$$\left(\frac{\partial s}{\partial P}\right)_T \approx \frac{s(P_2, T_0) - s(P_1, T_0)}{P_2 - P_1} \ , \tag{7.98}$$

and

$$\left(\frac{\partial s}{\partial T}\right)_P \approx \frac{s(P_0, T_2) - s(P_0, T_1)}{T_2 - T_1} \ . \tag{7.99}$$

The sound speed squared can then be approximated as

$$a^2 \approx \left.\frac{\Delta P}{\Delta \rho}\right|_s = \frac{P_2 - P_1}{\rho(P_2, T_A) - \rho(P_1, T_B)} \ . \tag{7.100}$$

where

$$T_A = T_0 + \left(\frac{\partial T}{\partial P}\right)_s (P_2 - P_0) \ , \tag{7.101}$$

$$T_B = T_0 + \left(\frac{\partial T}{\partial P}\right)_s (P_1 - P_0) \ , \tag{7.102}$$

Note that all the quantities in the difference approximations are given as a function of temperature and pressure enabling the use of the 'TP' equilibrium option to find an equilibrium state or else in the case of frozen composition, direct evaluation of the thermodynamic properties. This is the method that is used in the Python module soundspeed_eq.

If the thermodynamic state has a single component or the composition is fixed, the frozen sound speed is defined as

$$a_{fr}^2 = \left(\frac{\partial P}{\partial \rho}\right)_{s,\ \mathbf{Y}} , \tag{7.103}$$

which can be numerically estimated using the finite difference approximation

$$a_{fr}^2 \approx \frac{P(\rho_0 + \Delta\rho, s_0,\ \mathbf{Y}) - P(\rho_0 - \Delta\rho, s_0,\ \mathbf{Y})}{2\Delta\rho} . \tag{7.104}$$

The evaluation of this formula does not involve equilibrium computations and can be evaluated by straightforward evaluation of states on the isentrope, which is implemented in the MATLAB soundspeed_fr.m and Python soundspeed_fr routines:

```
rho0 = density(gas);
T0 = temperature(gas);
P0 = pressure(gas);
s0 = entropy_mass(gas);
x0 = moleFractions(gas);
rho1 = 0.99*rho0;
set(gas,'Density',rho1,'Entropy',s0,'MoleFractions',x0);
p1 = pressure(gas);
rho2 = 1.01*rho0;
set(gas,'Density',rho2,'Entropy',s0,'MoleFractions',x0);
p2 = pressure(gas);
dpdrho_s = (p2 - p1)/(rho2 - rho1);
afrozen = sqrt(dpdrho_s);
set(gas,'Temperature',T0,'Pressure',P0,'MoleFractions',x0);
```


These algorithms for sound speed are independent of equation of state and will work for both ideal and real gas equations of state.

As discussed in Section 7.10, the frozen sound speed can be computed from the thermodynamic identity

$$\left(\frac{\partial P}{\partial \rho}\right)_s = \frac{c_p}{c_v}\left(\frac{\partial P}{\partial \rho}\right)_T . \tag{7.105}$$

For frozen composition in a real gas, this quantities can be computed from the ideal gas properties and departure functions, evaluating the derivative using finite differences. For an ideal gas the derivative simplifies to

$$\left(\frac{\partial P}{\partial \rho}\right)_{T,\mathbf{Y}} = RT . \tag{7.106}$$

Defining the frozen ratio of specific heats as

$$\gamma_f(T) = \frac{c_{p,\mathbf{Y}}(T)}{c_{v,\mathbf{Y}}(T)} , \tag{7.107}$$

we obtain the following alternative expressions for frozen sound speed.

$$a_f^2 = \gamma_f(T)RT = \gamma_f(T)\frac{P}{\rho} \tag{7.108}$$

This is the extension of the perfect gas expression $a^2 = \gamma RT$ with $\gamma =$ constant to the situation of variable thermal properties accounting for the specific heat dependence on temperature through $\gamma_f(T)$.

Grüneisen Coefficient

The Grüneisen parameter is defined as

$$\mathcal{G} = v \left(\frac{\partial P}{\partial e} \right)_v , \tag{7.109}$$

which can be transformed using thermodynamic identities to

$$= -\frac{v}{T} \left(\frac{\partial T}{\partial v} \right)_s , \tag{7.110}$$

$$= \frac{\rho}{T} \left(\frac{\partial T}{\partial \rho} \right)_s . \tag{7.111}$$

The simplest approach to numerical computation is to use finite differences to approximate the derivative on the isentrope

$$\left(\frac{\partial T}{\partial \rho} \right)_s \approx \frac{T(s, \rho + \Delta\rho) - T(s, v\rho - \Delta\rho)}{2\Delta\rho} . \tag{7.112}$$

and the computation of temperature as a function of entropy and specific volume (or mass density) is either at equilibrium or frozen composition. The MATLAB script gruneisen_fr.m (the Python routine is gruneisen_fr) that implements the equilibrium composition version is:

```
rho0 = density(gas);
P0 = pressure(gas);
T0 = temperature(gas);
s0 = entropy_mass(gas);
x0 = moleFractions(gas);
rho1 = 0.99*rho0;
set(gas,'Density',rho1,'Entropy',s0,'MoleFractions',x0);
equilibrate(gas,'SV');
t1 = temperature(gas);
rho2 = 1.01*rho0;
set(gas,'Density',rho2,'Entropy',s0,'MoleFractions',x0);
equilibrate(gas,'SV');
t2 = temperature(gas);
dtdrho = (t2 - t1)/(rho2 - rho1);
rho = (rho1 + rho2)/2.;
t = (t1+t2)/2.;
G_eq = dtdrho*rho/t;
set(gas,'Temperature',T0,'Pressure',P0,'MoleFractions',x0);
```


Another method of computing the Grüneisen parameter is by using thermodynamic identities (Denbigh, 1981, Sec. 2.10) to transform the derivatives to use temperature and volume as the independent variables.

$$\mathcal{G} = v \left(\frac{\partial P}{\partial e} \right)_v , \tag{7.113}$$

$$= v \left(\frac{\partial P}{\partial T} \right)_v \left(\frac{\partial T}{\partial e} \right)_v , \tag{7.114}$$

$$= v \frac{\left(\frac{\partial P}{\partial T} \right)_v}{\left(\frac{\partial e}{\partial T} \right)_v} . \tag{7.115}$$

The denominator is the specific heat at constant volume

$$c_v = \left(\frac{\partial e}{\partial T}\right)_v , \tag{7.116}$$

and the numerator can be expressed (Denbigh, 1981, Sec. 2.10) as

$$\left(\frac{\partial P}{\partial T}\right)_v = -\frac{\left(\frac{\partial v}{\partial T}\right)_P}{\left(\frac{\partial v}{\partial P}\right)_T} . \tag{7.117}$$

The Grüneisen parameter can be expressed as

$$\mathcal{G} = -\frac{v}{c_v}\left(\frac{\partial P}{\partial v}\right)_T \left(\frac{\partial v}{\partial T}\right)_P . \tag{7.118}$$

The Grüneisen parameter can be related to other thermodynamic properties using the thermodynamic identity (Denbigh, 1981, Sec. 2.10)

$$c_p - c_v = -T\left(\frac{\partial P}{\partial v}\right)_T \left(\frac{\partial v}{\partial T}\right)_P^2 . \tag{7.119}$$

Subsituting the alternative definition (7.118), we obtain the following identity

$$\frac{c_p}{c_v} - 1 = \mathcal{G}\frac{T}{v}\left(\frac{\partial v}{\partial T}\right)_P . \tag{7.120}$$

Simplfying this with the definition (7.78) we obtain the final version of the relationship between γ and $\mathcal{G}$.

$$\gamma - 1 = \mathcal{G}\cdot\left[\frac{T}{v}\left(\frac{\partial v}{\partial T}\right)_P\right] . \tag{7.121}$$

The last two expressions are valid for both frozen and equilibrium compositions; the term in brackets in (7.121) is one for frozen conditions. The derivatives will need to be evaluated numerically if the equilibrium constraint applies. If the derivatives are evaluated at fixed composition, then substantial simplification occurs for an ideal gas.

$$\frac{1}{v}\left(\frac{\partial v}{\partial T}\right)_P = \frac{1}{T} \qquad \text{Frozen composition} , \tag{7.122}$$

$$-\frac{1}{v}\left(\frac{\partial v}{\partial P}\right)_T = \frac{1}{P} \qquad \text{Frozen composition} . \tag{7.123}$$

At fixed composition, the constant volume specific heat can be expressed in terms of the ratio of specific heats γ and the gas constant R

$$c_{v,f} = \frac{R}{\gamma_f - 1} \qquad \text{Frozen composition} , \tag{7.124}$$

$$\gamma_f = \frac{c_p}{c_v} \qquad \text{Frozen composition} . \tag{7.125}$$

Considering the frozen case, the Grüneisen parameter for an ideal gas can be expressed as

$$\mathcal{G}_f = \gamma_f - 1 \qquad \text{Frozen composition} \tag{7.126}$$

This can be used as a check on the finite difference approximation for the frozen case. The equilibrium case requires evaluating the derivatives using finite different approximations. Some progress can be made analytically for an ideal gas by expanding the derivative and simplifying to obtain

$$\frac{T}{v}\left(\frac{\partial v}{\partial T}\right)_P = 1 + \sum_{i=1}^{n} \frac{\mathcal{W}}{\mathcal{W}_i}\left(\frac{\partial Y_i}{\partial T}\right)_P \ . \tag{7.127}$$

The last term vanishes for frozen conditions (consistent with the previous discussion) and is positive for equilibrium combustion products, with a value as large as 1.5 for dissociated combustion products. As a consequence the values of γ obtained from the Grüneisen parameter are smaller than expected based on the relationship (7.126) extended to equilibrium conditions.

Ratio of specific heats

The specific heats are defined in terms of the derivatives of internal energy e

$$c_v = \left(\frac{\partial e}{\partial T}\right)_v \ , \tag{7.128}$$

or enthalpy h

$$c_p = \left(\frac{\partial h}{\partial T}\right)_p \ . \tag{7.129}$$

These derivatives can be carried out either at frozen or equilibrium conditions. The frozen case can be evaluated directly form the mixture average specific heats and the differentiation for the equilibrium case is carried out numerically in demo_g.m.


```
% compute frozen specific heats from thermodynamic properties
set(gas,'T',T(i),'V',V);
equilibrate(gas, 'TV');
gamma_fr_thermo(i) = cp_mass(gas)/cv_mass(gas);
% compute equilibrium specific heats from properties and definition
% constant volume
set(gas,'T',T(i)*1.01,'V',V);
equilibrate(gas, 'TV');
U2 = intEnergy_mass(gas);
set(gas,'T',T(i)*0.99,'V',V);
equilibrate(gas, 'TV');
U1 = intEnergy_mass(gas);
CVEQ = (U2-U1)/(.02*T(i));
% constant pressure
set(gas,'T',T(i)*1.01,'P',P(i));
equilibrate(gas, 'TP');
H2 = enthalpy_mass(gas);
set(gas,'T',T(i)*0.99,'P',P(i));
equilibrate(gas, 'TP');
H1 = enthalpy_mass(gas);
CPEQ = (H2-H1)/(.02*T(i));
gamma_eq_thermo(i) = CPEQ/CVEQ;
```

The frozen versions are relevant to fluid dynamic simulations (e.g., nozzle flow) and idealized explosion models (e.g., ZND, CV or CP computations) which model chemical reactions using detailed chemical kinetic descriptions. The equilibrium versions are sometimes used to describe idealized models of processes that are sufficiently slow to be modeled as a sequence of equilibrium states.

The ratio of the specific heats are related to the slopes of the isentrope and isotherm in the $P-\rho$ plane by a thermodynamic identity (Denbigh, 1981, Sec. 2-1) that is valid for either equilibrium or frozen conditions.

$$\left(\frac{\partial P}{\partial \rho}\right)_s = \frac{c_p}{c_v}\left(\frac{\partial P}{\partial \rho}\right)_T , \tag{7.130}$$

Using the definition of the ratio of specific heats (7.78) this can be expressed as

$$\gamma = \frac{a^2}{\left(\frac{\partial P}{\partial \rho}\right)_T} , \tag{7.131}$$

For an ideal gas,

$$\left(\frac{\partial P}{\partial \rho}\right)_T = RT + RT\sum_{i=1}^{n}\frac{\mathcal{W}}{\mathcal{W}_i}\rho\left(\frac{\partial Y_i}{\partial \rho}\right)_T . \tag{7.132}$$

The last term vanishes for frozen conditions and is negative for equilibrium conditions (see Fig. 7.16) so that

$$\left(\frac{\partial P}{\partial \rho}\right)_{T,eq} \leq RT . \tag{7.133}$$

The consequences of these relationships are that the equilibrium sound speed is lower than the frozen sound speed as shown in Fig. 7.13. The deviation of a^2 from linear dependence on T is due to both the change in specific heat ratio and composition with temperature. For both frozen and equilibrium flow we have

$$a^2 = \frac{c_p}{c_v}RT\left[1+\sum_{i=1}^{n}\frac{\mathcal{W}}{\mathcal{W}_i}\rho\left(\frac{\partial Y_i}{\partial \rho}\right)_T\right] , \tag{7.134}$$

For frozen flow, this is the extension of the usual perfect gas relationship to an ideal gas with fixed composition.

$$a_{fr}^2 = \frac{c_{p,fr}(T)}{c_{v,fr}(T)}RT , \tag{7.135}$$

$$= \gamma_{fr}(T)RT . \tag{7.136}$$

For equilibrium flow, there is similar expression but with an additional term due to the shift in composition with temperature changes

$$a_{eq}^2 = \frac{c_{p,eq}(T)}{c_{v,eq}(T)}RT\left[1+\sum_{i=1}^{n}\frac{\mathcal{W}}{\mathcal{W}_i}\rho\left(\frac{\partial Y_i}{\partial \rho}\right)_T\right] , \tag{7.137}$$

$$= \gamma_{eq}(T)RT\left[1+\sum_{i=1}^{n}\frac{\mathcal{W}}{\mathcal{W}_i}\rho\left(\frac{\partial Y_i}{\partial \rho}\right)_T\right] . \tag{7.138}$$

An alternative interpretation of the ratio of specific heats is in terms of the nondimensional (logarithmic) slope of the isentrope in pressure-density coordinates

$$\kappa = \frac{\rho}{P}\left(\frac{\partial P}{\partial \rho}\right)_s . \tag{7.139}$$

The origin of the approximation of the isentrope by a power law is based on the integrating this equation with $\kappa \approx$ constant $= k$. However, this is only valid over a limited range of thermodynamic states as shown in Fig. 7.14 and discussed in the beginning of this Appendix. The definition of κ can be rewritten as

$$\kappa = \gamma \cdot \left[\frac{\rho}{P}\left(\frac{\partial P}{\partial \rho}\right)_T\right] . \tag{7.140}$$

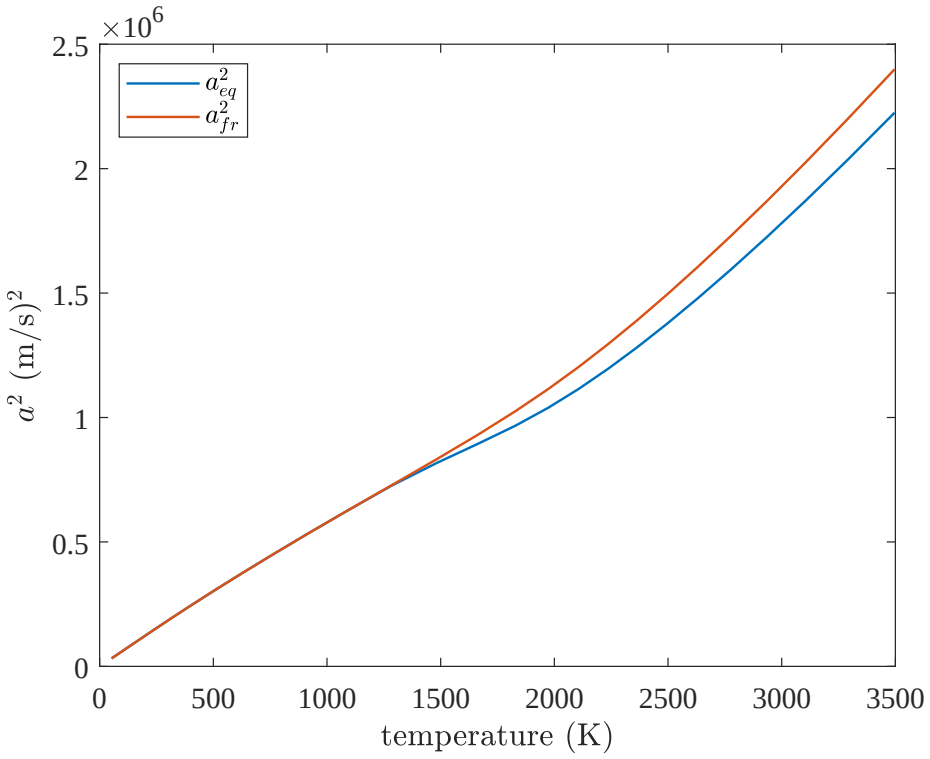

Figure 7.13: Frozen vs. equilibrium values of sound speed squared a^2 for isentropic expansion of combustion products of stoichiometric H_2-O_2 constant volume explosion.

The term in brackets is one for frozen flow and less than one for equilibrium conditions (Fig. 7.16a) so that the slopes of equilibrium isentropes at high temperature will be less than the ratio of specific heats.

In general $\mathcal{G}$, $\gamma - 1$, κ and c_p/c_v are functions of temperature and the frozen values are larger than the equilibrium values. As shown in Fig. 7.14a, the frozen values $\mathcal{G}_f = \gamma_f - 1 = \kappa_f - 1 = c_p/c_v - 1$ are all equal and show a nonmonotonic dependence on temperature. This is due to the competing processes of excitation of molecular degrees of freedom and dissociation of molecules to atoms with increasing temperature. In Fig. 7.14, value of γ was computed from (7.131) and the ratio of specific heats was computed from the definitions (7.128) and (7.129) using the appropriate composition constraint. Because these definitions are thermodynamically consistent, both frozen and equilibrium values of γ and c_p/c_v are identical to the precision of the computation and the curves overlap in Fig. 7.14. As shown in Fig. 7.14b, the equilibrium values of $\kappa - 1$ and $\mathcal{G}$ are significantly lower than $\gamma - 1$ at higher temperatures due to the temperature dependence (Fig. 7.16) of the derivatives in (7.121) and (7.140).

As shown in Fig. 7.15, at low temperatures, less than about 1200 K, the quantities $\gamma_{fr} = \kappa_{eq} = \gamma_{eq}$ are all equal and increase with decreasing temperature. At low temperatures, dissociation is unimportant (see Fig. 7.12) and composition can be considered frozen so that the specific heat varies only due to the population of molecular vibrational states associated with temperature. At intermediate temperatures, $1200 \leq T \leq 2000$, there is a substantial amount of dissociation and shifting composition in equilibrium effectively increases the heat capacity of the mixture and lowers the value of both $\kappa_{eq} - 1$ and $\gamma_{eq} - 1$ below $\gamma_{fr} - 1$. This effect is reflected in the variation of the functions shown in Fig. 7.16. With increasing temperatures above 2000 K, the mixture becomes progressively dominated by atoms resulting in an increase in the value of γ_{eq}. At 3500 K, the mixture is mostly atoms so that the frozen and equilibrium values of γ become equal.

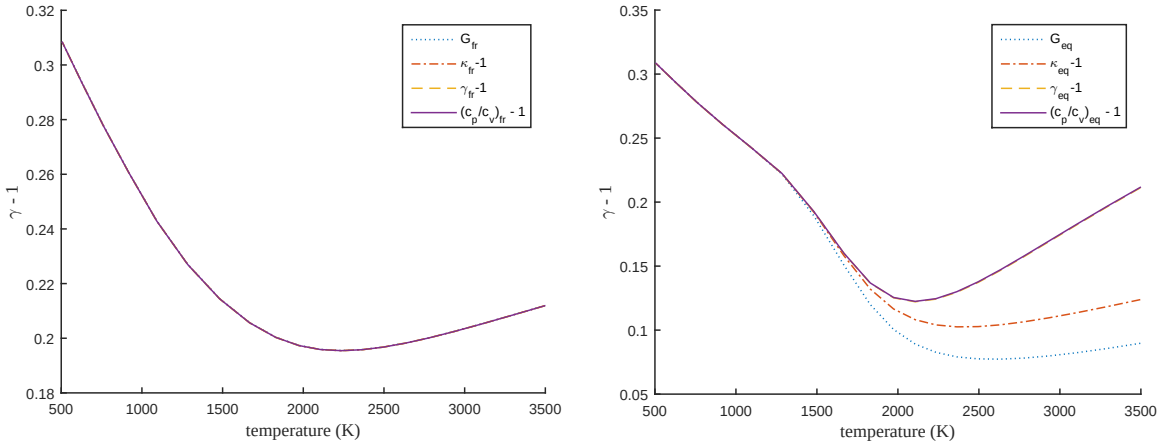

(a) frozen (b) equilibrium

Figure 7.14: Frozen vs. equilibrium values of γ -1 and κ - 1 for isentropic expansion of combustion products of stoichiometric H_2-O_2 constant volume explosion.

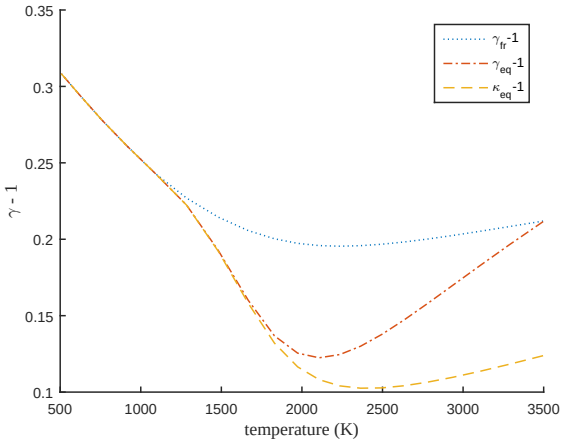

Figure 7.15: Frozen vs. equilibrium values of γ -1 and κ - 1.

7.11 Shock Tube Simulation

The classical shock tube consists of a high-pressure driver section separated by a diaphragm (metal or plastic sheet) from a low pressure driven section. Rupture of the diaphragm results in the propagation of a shock wave into the driver section and an expansion into the driven section, see Fig. 7.17. For an idealized shock tube, the diaphragm ruptures instantaneously and the conditions at states 2 and 3 as well as the shock strength can be computed by considering these regions as uniform until the waves have reflected from the far end of the tube and disturb the uniformity of states 2 and 3. This approximation is reasonable and be used to estimate the strength (Mach number or speed) of the shock wave in real shock tubes for locations sufficiently far from the diaphragm.

Idealized shock tube performance can be computed by numerically implementing simple wave solutions using the pressure-velocity matching method. For perfect gases in the driver and driven sections, the solution for the shock Mach number can be obtained analytically as a function of the ratio of specific heats of each gas, the ratio of initial sound speed a_4/a_1 in the driver and driven section, and the pressure ratio P_4/P_1. The solution (Appendix A.11) can be obtained analytically in this cases.

For strong shock waves and expansion from hot driver gases, realistic solutions for shock and expansion

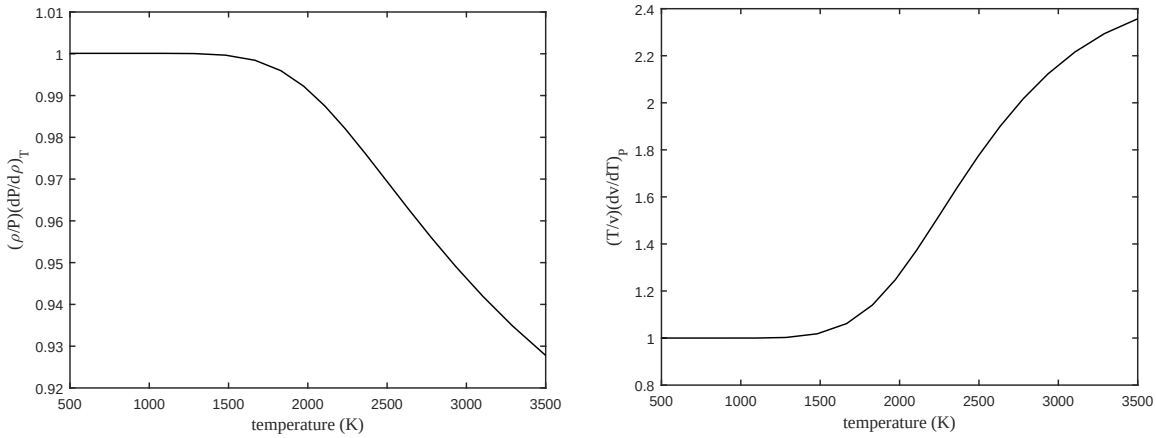

(a) (b)

Figure 7.16: (a) Equilibrium value of the function $(\rho/P)(dP/d\rho)_T$. (b) Equilibrium value of the function $(T/v)(dv/dT)_P$.

states require realistic thermochemistry using equilibrium solutions for the composition. This is implemented in the demonstration program demo_ShockTube.m and demo_ShockTube.py. There are four driver situations that have been implemented in the program.

1. Cold gas. This is the conventional shock tube situation in which the driver is just pressurized gas. The driver gas could be warm but in many cases it is cold, i.e., the same temperature as the driven gas.
2. Hot gas. The gas is hot and generated by a rapid combustion process, approximated as constant-volume, adiabatic, complete combustion.
3. Forward detonation. An ideal detonation wave propagating toward the diaphragm at the CJ speed.
4. Reverse detonation. An ideal detonation wave starting at the diaphragm and propagation away at the CJ speed.

In all cases, the solution is constructed by first computing the *wave curves* that represent the $P(u)$ relationship for the states behind the shock waves in the driver and expansion in the driven section. The $P(u)$ relationship for the shock wave is constructed using the `postshock` routines described in Section 6.1 and computed postshock pressure and density as a function of shock speed U_s.

$$P_2 = P_2(U_s) \tag{7.141}$$

$$\rho_2 = \rho(U_s) \tag{7.142}$$

$$u_2 = U_s(1 - \frac{\rho_1}{\rho_2}) \tag{7.143}$$

The$P(u)$ relationship for the expansion wave follows the development given in Section 7.1. For the left-propagating expansion shown in Fig. 7.17, the C^+ Riemann invariant across the wave provides the relationship

$$\frac{\mathrm{d}P}{\rho a} = -\mathrm{d}u \; . \tag{7.144}$$

Integration along an isentrope provides the required $P(u)$ relationship

$$u = -\int_{P_4}^{P} \frac{\mathrm{d}P}{\rho a} \; . \tag{7.145}$$